1.3.6 Thermal transport, thermoelectricity and quantum thermodynamics in nanostructures

Thermoelectricity has recently received mich attention owing to the constant demand for new effective ways of energy conversion. Increasing the efficiency of thermoelectric materials, heat engines and refrigerators at the nanoscale is one of the main challenges for several different technological applications. Moreover, improving thermal management at low temperatures is crucial for nanoscale quantum technologies.

One of the keys to success in this field is the ability to modulate, control, and route heat and charge currents, ideally achieving their separate control. This is however by no means obvious as the charge and (the electronic contribution to) the heat are transported by the same carriers. In two-terminal systems, within the linear response regime, electrical and thermal currents are strictly interrelated, as manifested by the emergence at low enough temperatures of the Wiedemann-Franz (WF) law. In this respect, multi-terminal devices, so far poorly investigated, offer the possibility to 'decouple' energy and charge flows, and improve thermoelectric efficiency.
In this context we have developed a general formalism for linear-response multi-terminal thermoelectric transport. In particular, we have worked out analytical expressions for the efficiency at maximum power in the three-terminal case. By means of two simple quantum-dot-based non-interacting models, we have shown that a third terminal can be useful to improve the thermoelectric performance of a system with respect to the two-terminal case [1].

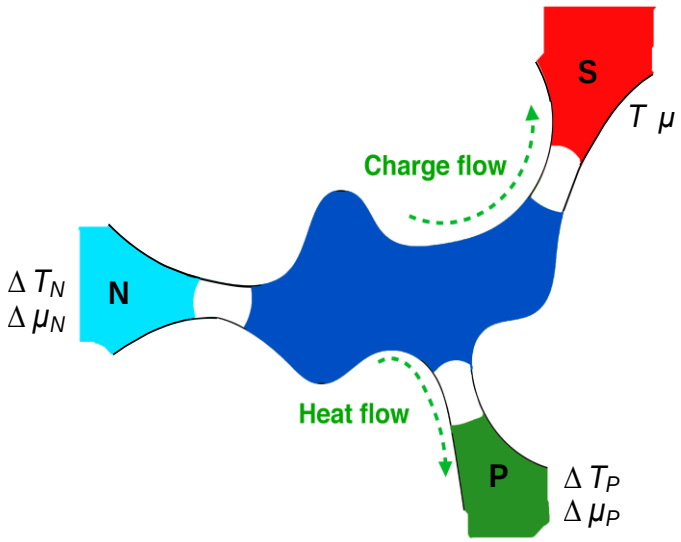

Figure 1. The heat-charge current separation scheme. A generic conductor is connected to three reservoirs labelled by the letters S (superconducting lead), P (voltage probe), and N (normal metal lead). The reservoir S is the reference for the temperature T and the chemical potential μ. A temperature (chemical potential) difference ΔT_N and ΔT_P ($\Delta\mu_N$ and $\Delta\mu_P$) is present in reservoir N and P, respectively. As indicated by the arrows, only charge flows inside lead S whereas only heat flows inside lead P.

Furthermore, we have analyzed the performance of a thermal machine that allows for the spatial separation between heat and charge currents. It is realized by connecting a conductor to a superconducting lead, a voltage probe, and a normal lead (see Fig. 1). We have shown that in the low temperature limit such system violates the WF law and allows, to some extent, an independent control of electrical conductance, thermal conductance, and thermopower [2]. We have thus shown, on statistical grounds, that the system exhibits much larger values of the power factor Q and of the figure of merit ZT (one order of magnitude), with respect to the two-terminal counterpart (see Fig. 2).

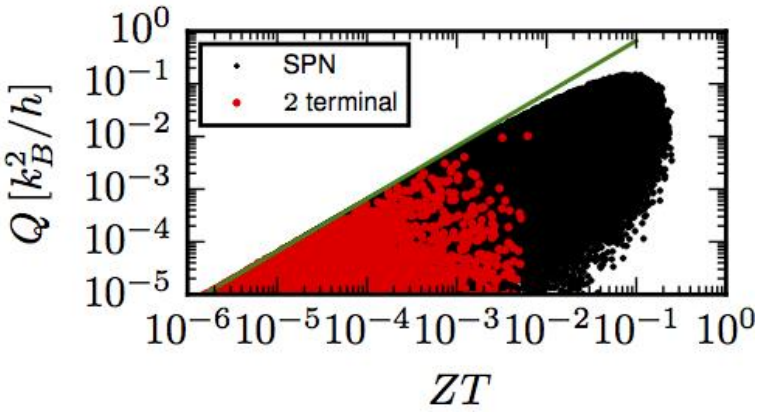

Figure 2. Correlation between the power factor Q and the figure of merit ZT relative to systems consisting of three quantum dots for the SPN setup (black points) and the two-terminal setup (red points). The green curve corresponds to the bound given by the unitarity of the scattering matrix, and sets a maximum value for Q as a function of ZT. The plot shows that for the SPN setup both Q and ZT are one order of magnitude larger with respect to the corresponding values for the two-terminal system. The plot refers to 10^5 Hamiltonian realizations, taking the couplings with the reservoirs P and N equal to $10^3\ k_BT$.

Heat-to-work conversion based on thermoelectricity promises an enhanced efficiency as a consequence of the reduction of the phonon contribution to thermal conductance in disordered nanostructures and of the "energy filtering" effect that can result from confinement and quantum effects. A heat engine composed of a quantum dot (QD) is a paradigmatic example, since it is characterized by a spectrum of discrete levels which maximizes energy filtering. In this context, we have theoretically studied the thermoelectric properties and heat-to-work conversion performance of a multilevel QD in a multi-terminal configuration within the Coulomb blockade regime [4]. In the linear response and for low temperatures, we have derived analytical expressions for all transport coefficients, for the power factor Q and for the figure of merit ZT (which controls the maximum efficiency and the efficiency at maximum power). We have found the specific values of the gate voltage, which only depend on temperature, for which Q and ZT are simultaneously maximized (see Fig. 3). The regime beyond the linear response has been analyzed numerically. In this case, the efficiency at maximum power develops peaks which approach the Carnot efficiency for large temperature differences. Remarkably, the maximum power, normalized to its peak value, only slightly depends on the temperature bias and can be well approximated by the analytic expression obtained for the linear response regime. Moreover, we have found that efficiency at maximum power and maximum power take approximately their peak values simultaneously, under the same conditions found for the linear response.

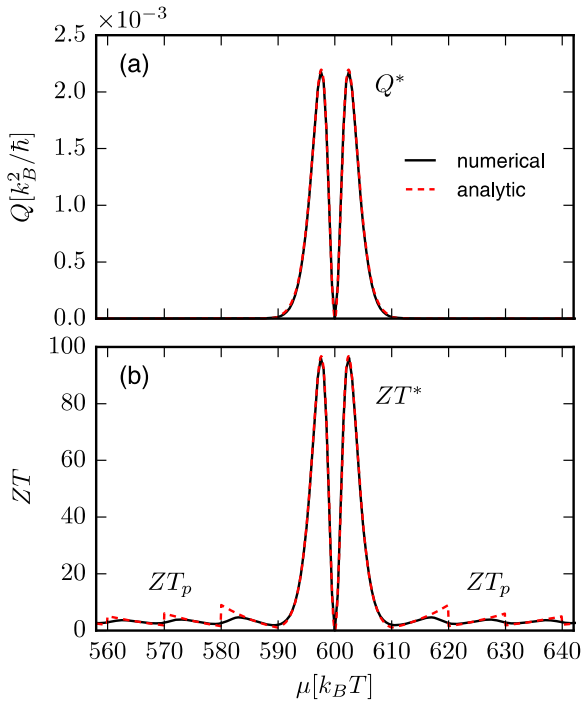

Figure 3. Power factor Q (a) and figure of merit ZT (b) are plotted as a function of the electrochemical potential μ (gate voltage) for a multi-level QD. For both quantities, the analytical quantum limit is plotted as a red dashed curve, while the numerically calculated result is plotted as a black solid curve. All curves are calculated for a charging energy $\boldsymbol{E_C = 50\, k_B T}$, level spacing $\boldsymbol{\Delta E = 10\, k_B T}$, and coupling energy of the tunnel barriers defining the QD given by $\boldsymbol{\hbar\Gamma = 0.01\, k_B T}$, $\boldsymbol{T}$ being the reference temperature. $\boldsymbol{Q^* \simeq 0.22\frac{\Gamma k_B}{T}}$ is the peak value of $\boldsymbol{Q}$, $\boldsymbol{ZT^* \simeq 0.44\frac{exp(\frac{\Delta E}{k_B T})}{(\frac{\Delta E}{k_B T})^2}}$ is the figure of merit peak value, and $\boldsymbol{ZT_p = 3}$ (for large $\boldsymbol{p}$) is the value of $\boldsymbol{ZT}$ of the secondary peaks.

In conclusion, we have found that Coulomb interactions dramatically increase ZT (by strongly suppressing the thermal conductance) and the non-linear-response efficiency at maximum power (pushing it above the Curzon-Alhborn limit).

More recently we have considered electronic thermal transport in systems composed of two metallic islands (MIs) or quantum dots (QDs) that are electrically isolated (but capacitively coupled) and placed in the two circuits (the drive and the drag) of a three- or four-electrode setup. In the latter setup we study the thermal drag effect when the system is biased, for example by a temperature ΔT, on the drive circuit, while no biases are present on the drag circuit [5]. The three-electrode setup is analyzed as a simple implementation of an autonomous refrigerator, a system that uses heat as a resource to achieve refrigeration [6]. We have also applied our theoretical approach to model three different experiments, the first regarding the measurement of thermovoltage in MIs [7], the second one regarding the occurrence of an apparent violation of the second law of thermodynamics in the statistics of work extraction from a MI [8] (see Fig. 4), and the third one regarding the thermoelectric response of a QD fabricated using the technology of heterostuctured nanowires. In the latter, a precise measurement of the Seebeck coefficient was obtained and – thanks to modelling – a precise estimate of the thermal transport and conversion efficiency was achieved (with a figure of merit up to ZT=35 at 30K).

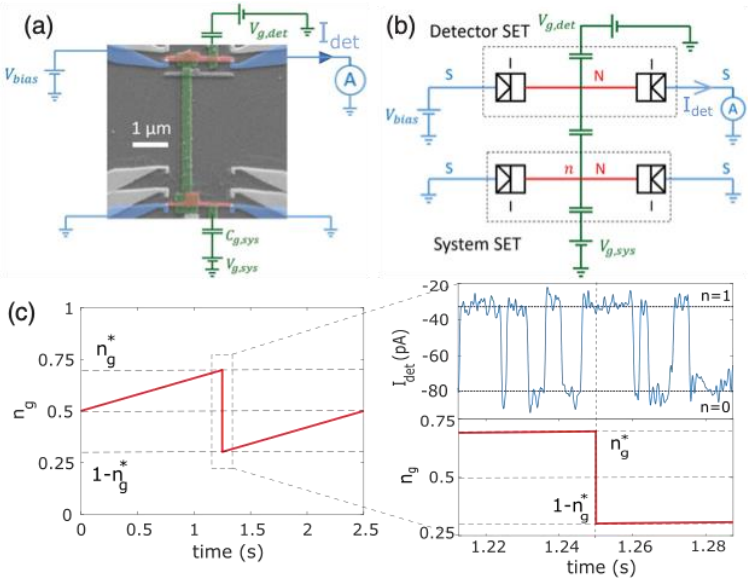

Figure 4. (a) Scanning electron micrograph of the single-electron transistor (SET) capacitively coupled to a voltage-biased detector SET. Leads (blue) made of superconducting aluminum are coupled through oxide (tunnel) barriers to the copper (red) island. (b) Electrical circuit representation. (c) Protocol used to maximize work extraction, with a zoom on the detector SET output current under system driving, around the quench event.

Finally, we have investigated nonlocal thermoelectricity in a hybrid superconducting nanosystem, such as the Cooper pair splitter (CPS), implemented using a double quantum dot in a nanowire system coupled to a superconductor (see Fig. 5a) [9]. Fig. 5b shows the thermodynamic efficiency of the nonlocal Seebeck (blue curve) and Peltier (red curve) effect. We have found that the nonlocal thermoelectric response is a direct consequence of the nonlocal splitting of the Cooper pair into the two quantum dots.

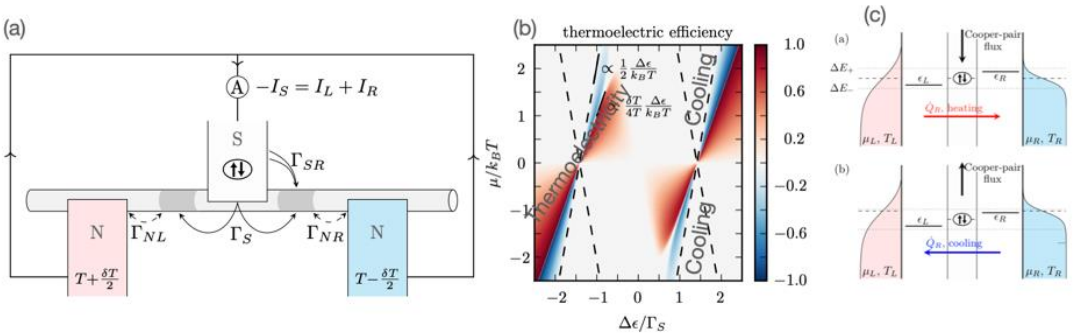

Figure 5. (a) Nanowire-based CPS to investigate nonlocal thermoelectric effects. The thermal gradient is applied to the normal metal leads N and the current is collected in the superconducting terminal. (b) Themoelectrical efficiency of the CPS in the plane of the level detuning and bias potential applied to the normal metal leads. In blue and red are shown the thermodynamical efficiency and the COP respectively for the nonlocal Seebeck and Peltier effect. (c) Energy scheme for the nonlocal heat pump (upper panel) and cooler (lower panel), depending on the direction of the driving current in the superconductor. The direction of the heat flows depends only on the gate configuration in the double quantum dots, thus realizing an electrically controlled nonlocal thermal router.

References

[1] F. Mazza, R. Bosisio, G. Benenti, V. Giovannetti, R. Fazio, F. Taddei, *Thermoelectric efficiency of three-terminal quantum thermal machines*, New J. Phys. **16**, 085001 (2014).

[2] F. Mazza, S. Valentini, R. Bosisio, G. Benenti, V. Giovannetti, R. Fazio, F. Taddei, *Separation of heat and charge currents for boosted thermoelectric conversion*, Phys. Rev. B **91**, 245435 (2015).

[3] R. Bosisio, S. Valentini, F. Mazza, G. Benenti, R. Fazio, V. Giovannetti, F. Taddei, *Magnetic thermal switch for heat management at the nanoscale*, Phys. Rev. B **91**, 205420 (2015).

[4] P.A. Erdman, F. Mazza, R. Bosisio, G. Benenti, R. Fazio, F. Taddei, *Thermoelectric properties of an interacting quantum dot based heat engine*, Phys. Rev. B **95**, 245432 (2017).

[5] B. Bhandari, G. Chiriacò, P.A. Erdman, R. Fazio, F. Taddei, *Thermal drag in electronic conductors*, Phys. Rev. B **98**, 35415 (2018).

[6] P.A. Erdman, B. Bhandari, R. Fazio, J. P. Pekola, F. Taddei, *Absorption refrigerators based on Coulomb-coupled single-electron systems*, Phys. Rev. B **98**, 45433 (2018).

[7] P.A. Erdman, J.T. Peltonen, B. Bhandari, B. Dutta, H. Courtois, R. Fazio, F. Taddei, J.P. Pekola, *Nonlinear thermovoltage in a single-electron transistor*, Phys. Rev. B **99**, 165405 (2019).

[8] O. Maillet, P.A. Erdman, V. Cavina, B. Bhandari, E.T. Mannila, J.T. Peltonen, A. Mari, F. Taddei, C. Jarzynski, V. Giovannetti, J.P. Pekola, *Optimal probabilistic work extraction beyond the free energy difference with a single-electron device*, Phys. Rev. Lett. **122**, 150604 (2019).

[9] R. Hussein, M. Governale, S. Kohler, W. Belzig, F. Giazotto, A. Braggio, *Nonlocal thermoelectricity in a Cooper-pair splitter*, Phys. Rev. B **99**, 075429 (2019).